Looping Dynamics of Linear DNA Molecules and the Effect of DNA Curvature: A Study by Brownian Dynamics Simulation

Holger Merlitz, Karsten Rippe, Konstantin V. Klenin, and Jörg Langowski
Division Biophysics of Macromolecules, German Cancer Research Center (DKFZ), D-69120 Heidelberg, Germany

ABSTRACT A Brownian dynamics (BD) model described in the accompanying paper (Klenin, K., H. Merlitz, and J. Langowski. 1998. A Brownian dynamics program for the simulation of linear and circular DNA, and other wormlike chain polyelectrolytes. *Biophys. J.* 74:000–000) has been used for computing the end-to-end distance distribution function, the cyclization probability, and the cyclization kinetics of linear DNA fragments between 120 and 470 basepairs with optional insertion of DNA bends. Protein-mediated DNA loop formation was modeled by varying the reaction distance for cyclization between 0 and 10 nm. The low cyclization probability of DNA fragments shorter than the Kuhn length (300 bp) is enhanced by several orders of magnitude when the cyclization is mediated by a protein bridge of 10 nm diameter, and/or when the DNA is bent. From the BD trajectories, end-to-end collision frequencies were computed. Typical rates for loop formation of linear DNAs are $1.3 \cdot 10^3$ s^{-1} (235 bp) and $4.8 \cdot 10^2$ s^{-1} (470 bp), while the insertion of a 120° degree bend in the center increases this rate to $3.0 \cdot 10^4$ s^{-1} (235 bp) and $5.5 \cdot 10^3$ s^{-1} (470 bp), respectively. The duration of each encounter is between 0.05 and 0.5 μs for these DNAs. The results are discussed in the context of the interaction of transcription activator proteins.

INTRODUCTION

Many examples in transcription, replication, and recombination exist where DNA looping has been shown to be implicated in the function of DNA-binding proteins, for instance in the action of p53 (Stenger et al., 1994), Ultrabithorax protein (Beachy et al., 1993), EBNA1 protein of Epstein-Barr virus (Frappier et al., 1994; Frappier and O'Donnell, 1991; Su et al., 1991), NtrC (Rippe et al., 1997; Su et al., 1990; Wedel et al., 1990), AraC protein (Schleif, 1992), lac repressor (Krämer et al., 1987), and HU protein (Haykinson and Johnson, 1993). Numerous other examples have been described in the literature and reviews are given in Bellomy and Record (1990), Hochschild (1990), and Schleif (1992). Loop formation can be facilitated by DNA bending as shown for IHF-induced bending (Carmona and Magasanik, 1996; Moitoso de Vargas et al., 1989; Santero et al., 1992) or intrinsic bending of the DNA (Bracco et al., 1989; Lavigne et al., 1992).

Protein-protein interactions mediated by DNA looping are of particular importance for the transcription initiation process. The vast majority of genes in eukaryotes and also some genes in prokaryotes are controlled by activator proteins that bind far away from the promoter to DNA sequences designated as enhancers or upstream elements. Physical contact between the transcription machinery at the promoter and the regulating protein(s) at these sequences can be realized by DNA looping, leading to the initiation of transcription. One can classify the systems in which interaction through DNA looping plays a role according to the distance of the interaction. While in typical upstream elements the distance between the transcription factor binding site and the promoter is typically around 100–200 bp, other *cis*-acting regulatory regions, called enhancers, may be several thousands of basepairs away from the promoter. As outlined in Rippe et al. (1995), the effect of DNA bending and finite protein size on the interaction probability is most dramatic when the DNA length between the sites is of the order of 2 persistence lengths (300 bp) or less. For very distant sites, local bending or finite protein size does not influence the looping probability. An effect of DNA bending for large separation distances is only expected when the two interacting sites are in a superhelical context, because the bend defines the position of the end loop of the superhelix (Klenin et al., 1995; Laundon and Griffith, 1988; Yang et al., 1995).

Different experimental techniques have been used to study DNA loop formation in vitro and in vivo. The classical method to measure DNA looping in vitro, cyclization kinetics, was pioneered by Shore and Baldwin (1983) and Shore et al. (1981), and has later been applied to many other related problems. In addition, in a variety of systems periodic variations in gene activity with the distance between activator binding site and promoter, or two repressor sites, have been reported (Bellomy et al., 1988; Borowiec et al., 1987; Mossing and Record, 1986). From these studies loop formation probabilities and DNA elastic constants could be estimated in vivo.

With the wealth of available in vitro and in vivo data, it becomes important to develop a consistent physicochemical description of the process by which two distant DNA sites interact with one another through space. Such a description represents a formidable theoretical problem if one wants to

Received for publication 19 June 1997 and in final form 3 November 1997.

Address reprint requests to Dr. Jörg Langowski, Deutsches Krebsforschungszentrum, Abt. Biophysik der Makromoleküle (0830), Postfach 101949, D-69009 Heidelberg, Germany. Tel.: 49-6221-423390; Fax: 49-6221-423391; E-mail: joerg.langowski@dkfz-heidelberg.de.

Dr. Merlitz's present address is Max-Planck-Institut für Kernphysik, D-69117 Heidelberg, Germany.

Dr. Klenin's present address is TRINITI, Troitsk, Moscow region, Russia.

0006-3495/98/02/773/07 $2.00

deal with the most general case, i.e., calculating the probability of interaction of two ends of DNA fragment at any arbitrary relative orientation and distance—parameters that would be implied by the geometry of the protein bridge—and for any type of DNA structure and flexibility for the sequence between the contacting ends.

Enhancing the theoretical description by incorporating more structural details of the DNA-protein loop is only possible by a numerical treatment of the problem. A description of the DNA chain by a model where groups of basepairs are considered as rigid units and their interaction is given by harmonic bending, twisting, and stretching potentials has proven very successful in describing the structure and dynamics of linear and superhelical DNAs. Such a model may be used to calculate thermodynamic equilibrium structural ensembles through Monte Carlo procedures (Bednar et al., 1994; Gebe et al., 1995; Gebe and Schurr, 1996; Klenin et al., 1995, 1991; Kremer et al., 1993; Langowski et al., 1994; Rybenkov et al., 1997a,b; Vologodskii et al., 1992) and also to describe the dynamics of DNA on micro-to-millisecond time scales by Brownian dynamics (BD) procedures (Allison et al., 1989, 1990; Chirico and Langowski, 1992, 1994, 1996; Ehrlich et al., 1997; Heath et al., 1996). Other types of models, notably elastic-chain models using finite-element or spline function approaches (Martino and Olson, 1997; Olson, 1996; Olson et al., 1993; Schlick and Olson, 1992; Yang et al., 1995; Zhang et al., 1994) have been used to calculate structural properties of large DNAs, but these models, which exclude thermal fluctuations, are not adequate for computing thermodynamic properties (Langowski et al., 1996).

By using a BD model we have recently obtained first data on the enhancement of intramolecular interaction in DNA by looping under conditions where the two DNA ends were connected by a 10-nm protein bridge and an optional bend was inserted in the chain (Rippe et al., 1995). Here we present an analysis of the *kinetics* of the looping process and an extension of the first calculations to other biologically interesting cases.

METHODS

Brownian dynamics model

The BD model used here is described in the accompanying paper (Klenin et al., 1998). The simulations were performed using a statistical segment length of 100 nm [i.e., persistence length of 50 nm (Hagerman, 1988)], at 25°C and in 0.1 M NaCl. The length of the unit segment in the model was 3.18 nm, corresponding to a spherical bead encompassing 9.35 bp. A touching-beads chain with this choice of bead diameter is known to describe the hydrodynamic diameter of DNA quantitatively (Hagerman and Zimm, 1981). The simulation time step was $\Delta t = 0.2$ ns, and the second-order algorithm was used.

End-to-end contact probabilities are given in the form of the *j*-factor $j_M(r)$, which we define here as the concentration of one chain end in a spherical shell of radius r around the other end. The correct torsional alignment of the two ends/sites can be important for biologically functional protein-protein contacts, but was not considered here. The concentrations given by j_M are equivalent to the same concentration of a species free in solution. If the torsional orientation of the sites on the DNA is favorable, the interaction is facilitated as compared to interactions free in solution; for an unfavorable orientation the interaction will be inhibited. Thus the j_M values presented should be considered as averages. For protein-protein interactions an unfavorable torsional alignment may reduce j_M as much as 10-fold if the length of the intervening DNA is between 60 and 130 bp (Haykinson and Johnson, 1993), and as much as fivefold for a DNA length of 130–200 bp (Law et al., 1993). With longer distances the effect disappears, and should be hardly noticeable above 800 bp (Rippe et al., 1995).

The simulations were done with chains up to 160 nm length. To obtain the end-to-end distance distribution for which hydrodynamic interactions (HI) can be omitted, simulation times of $t_{sim} = 50$ ms were reached. The simulations of the chain dynamics to obtain the first entrance times needed HI, and hence were more time-consuming. Here only simulations with $t_{sim} = 10$ ms were conducted. The autocorrelation times with respect to the end-to-end distance for the fragments studied were in the order of 10 μs. Starting from a random position on the trajectory, the time until the next entrance into a sphere with $r \leq 10$ nm around one end was determined. This procedure was repeated ~800–1000 times for each trajectory of 10 ms to sample the independent conformations. The data obtained were categorized with respect to the contact times to obtain a discrete function where the number of molecules versus time to reach the conformation with $r = 10$ nm is given.

RESULTS

The end-to-end contact probability of DNA chains is shown in Fig. 1. An analytical solution has been given by Shimada and Yamakawa (1984) for the case when the two chain ends have to come into direct contact to form a loop (*dashed curve* in Fig. 1 *A*). While the agreement between the simulated and the analytical values is satisfactory. Monte Carlo simulations reported by Hagerman and Ramadevi (1990) showed better agreement with the Shimada-Yamakawa (SY) expression. One reason might be that both the Hagerman-Ramadevi and the SY work do not take into account excluded volume. It is well conceivable that for intermediate fragment lengths where the *j*-factor is near its maximum excluded volume effects will lower the cyclization probability to some extent. At any rate, the deviation between our BD data and the SY expression is small compared to the difference to the experimental cyclization probabilities reported by Shore et al. (1981) (*black squares* in Fig. 1 *A*). It is clearly seen that our values constitute an upper limit to the experimental data; this is because we did not take into account effects of torsional or axial orientation of the DNA ends. As discussed above, torsional orientation effects might either increase or decrease j_M as compared to the value computed here; however, the requirement of correct axial orientation will always lower j_M (for small rings correct axial alignment at the ends requires extra bending).

Fig. 1 *B* shows the effect of a bound protein and chain bending on the *j*-factor. For short fragments the looping probability is increased by an order of magnitude by allowing end-to-end contact at a distance of $r = 10$ nm instead of $r = 0$. This corresponds to the dimensions of a typical protein-protein bridge between two DNA segments, e.g., lac repressor tetramer binding two operator sites (Lewis et al., 1996) or an enhancer bridged to the promoter by a contact between a transcription factor and the RNA polymerase

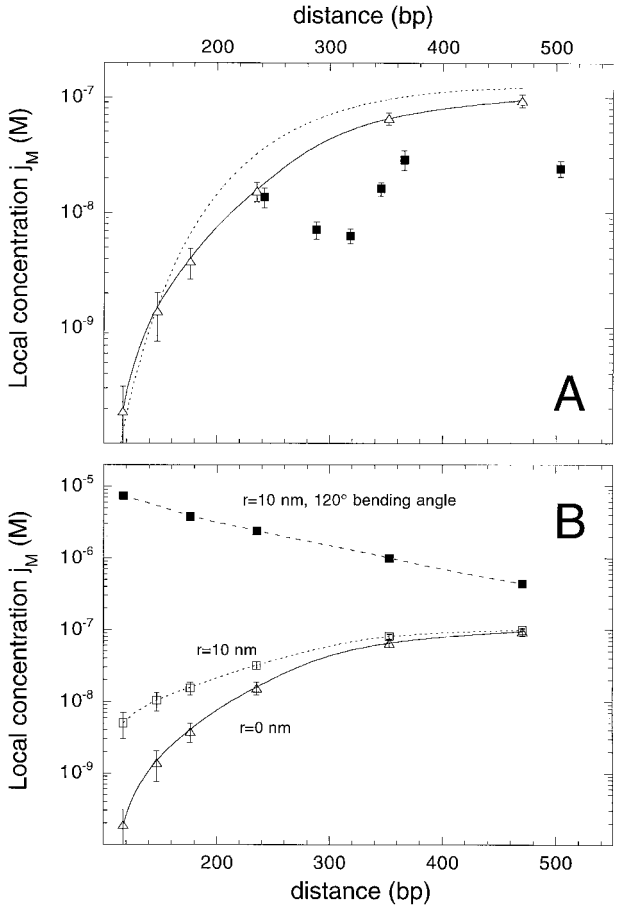

FIGURE 1 Local concentration j_M for linear DNA fragments of 120 (40 nm), 150 (50 nm), 240 (80 nm), 350 (120 nm), and 470 (150 nm) basepairs. (*A*) Local concentration j_M at $r = 0$ determined from the Brownian dynamics simulation (—△—) or calculated according to Shimada and Yamakawa (1984) (···). (■), experimental j_M values determined by Shore et al. (1981). (*B*) Comparison of j_M at $r = 0$ (—△—), at $r = 10$ nm (—□—), and at $r = 10$ nm (–■–) with a central bending angle of 120°.

[e.g., NtrC-RNA polymerase-σ^{54} holoenzyme (Rippe et al., 1997)].

At DNA lengths >350 bp there is no significant difference between the curves for $r = 0$ nm and for $r = 10$ nm. At 150 bp we have a 10-fold higher value at $r = 10$ nm as compared to $r = 0$ nm. However, the concentration at this point is still lower by a factor of 10 than at ~500 bp, where the maximum of j_M is located for linear DNAs with no specific bends. In connection with the upstream activation elements of eukaryotic promoters, the question arises why these are generally located 100–200 bp away from the promoter if the local concentration at the promoter would be higher at a separation distance of 500 bp. A possible explanation for this observation could be that the kinetics of loop formation favor shorter separation distances (see below) and/or that DNA curvature increases the local concentration j_M. The latter effect was studied by introducing a 120° bend in the center of the DNA that increases the looping probability dramatically as compared to the straight 120-bp fragment at $r = 10$ nm. The bent fragment's *j*-factor is more than three orders of magnitude higher. In contrast to the straight fragment where j_M ($r = 10$ nm) increases by about an order of magnitude from 120 to 470 bp, the contact probability decreases slightly with length for the bent fragment. The difference between the bent and straight cases, as well as the $r = 0$ case, becomes smaller with increasing length and disappears for DNA lengths > 1000 bp (data not shown).

The results presented in Fig. 1 *B* demonstrated that DNA bending can dramatically increase the interactions between proteins that are separated by 100–200 bp as, for example, between activator proteins bound at upstream elements and proteins at the promoter. In this context it is noteworthy that the general transcription factor TBP introduces an 80° bend into the DNA at a position located ~30 bp upstream of the transcription start (Kim et al., 1993a,b). In order to study this case in more detail we have conducted simulations on a 51-nm linear fragment (150 bp) where the position of the ends would correspond to the transcription start site and the position of an upstream element. Introduction of an 80° bend ~⅕ (= 30 bp) away from one end as introduced by TBP leads to only a 10-fold increase of j_M, whereas the same 80° bend located in the center of the fragment increases j_M several hundredfold as compared to the unbent DNA. We conclude that asymmetrically located bends are much less effective in promoting interactions by DNA looping, and it appears therefore less likely that the TBP-induced bend alone plays a dominant role in mediating interactions with upstream elements.

However, it could be possible that additional intrinsic curvature of the DNA between the two sites is also present. This notion is supported in a recent analysis of the intrinsic curvature observed in the region between the upstream element and promoter of 200 eukaryotic sequences, where a significant increase of curvature has been detected (Schätz and Langowski, in preparation). Therefore, also the synergistic effect of two bends was examined and the corresponding data are presented in Fig. 2. The data show that a TBP bend in conjunction with additional intrinsic DNA curvature could have a much larger effect on the interaction probability.

In Figs. 1 and 2 we have calculated j_M for the interaction between the two ends of linear DNA. However, the relevant situation in vivo is the interaction between two sites located on a longer DNA fragment. To compare the contact probability we have determined the dependence of j_M on r for the ends of an 80-nm DNA and for two sites separated by 80 nm that were located in the center of a 160-nm DNA (Fig. 3). Both DNAs had a central 120° bending angle. Significant differences occur only at the short separation distances, i.e., $r < 15$ nm. It can be seen from inspection of Fig. 3 that at $r = 10$ nm the value of j_M for end-to-end interactions is two times higher ($2.9 \cdot 10^{-6}$ M versus $1.5 \cdot 10^{-6}$ M) with even larger differences at smaller values of r.

The data presented in Figs. 1–3 reflect the equilibrium conformation of the DNAs analyzed. However, we can also

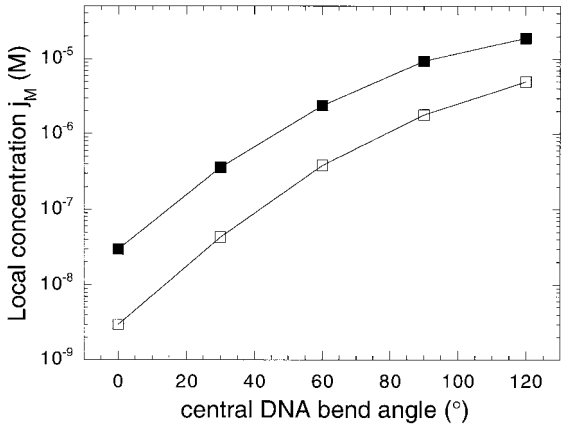

FIGURE 2 Local concentration j_M at $r = 10$ nm for a 51 nm (= 150 bp) long linear fragment. The fragment has a central DNA bend of the magnitude that is given on the x axis (—□—). The second curve (—■—) is for a DNA of the same length with an additional bend of 80° ~¼ from one end, which is to mimic the TBP-induced bend. The error bars are smaller than the size of the symbols.

determine the kinetics of DNA loop formation, since the BD simulations provide us with the dynamical evolution of the chain. For extracting the first-order rate constant of loop formation from the trajectory data, we selected a random starting point on the trajectory and measured the *first entrance time*, i.e., the time until the chain ends met within a distance of 10 nm. As described in the accompanying paper (Klenin et al., 1998), the number of statistically independent configurations with respect to the end-to-end distance, N_{eff}, is ~5000 for the 80-nm chain and 455 for the 160-nm chain in a 10-ms trajectory. We therefore collected $\sim N_0 = 1000$ samples from each trajectory, which is around N_{eff} for the chains studied. The first-order rate constant was then computed by treating cyclization as irreversible and plotting the number of "non-looped" samples N_{linear} against time:

$$N_{\text{linear}}(t) = N_0 - N_{\text{loop}}(t) \tag{1}$$

$N_{\text{loop}}(t)$ is the number of samples that have first entrance times $\leq t$. This is equivalent to treating the cyclization process as an irreversible first-order rate mechanism

$$\text{linear} \xrightarrow{k_{on}} \text{loop} \tag{2}$$

with the rate law

$$N_{\text{linear}}(t) = N_0 \exp(-k_{\text{on}}t) \tag{3}$$

Accordingly, we can fit the data obtained from Eq. 1 to the single exponential given in Eq. 3. This yields the cyclization rate constant k_{on}, and is shown in Fig. 4 for 80- and 160-nm fragments with and without a central 120° DNA bend. The values obtained for k_{on} are given in Table 1. To obtain the kinetic and equilibrium constants for loop formation we have to take into account that the dissociation of the

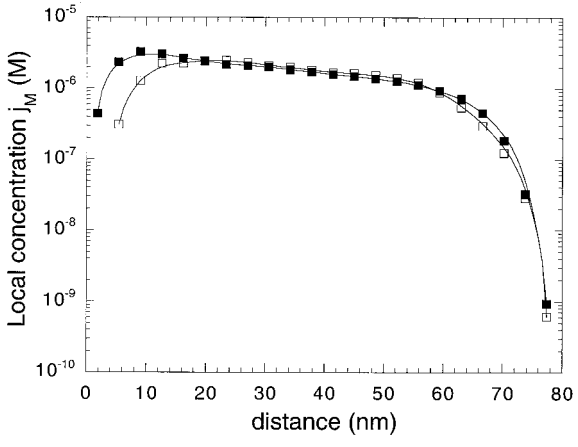

FIGURE 3 Comparison of $j_M(r)$ end-to-end interactions to site to site interactions. The value of j_M as a function of the separation distance r is given for the end-to-end distance of an 80-nm (240 bp) fragment (—■—) and for the two sites separated by 80 nm on a 160-nm fragment (—□—). Both DNAs had a central 120° bending angle. The error bars are smaller than the size of the symbols.

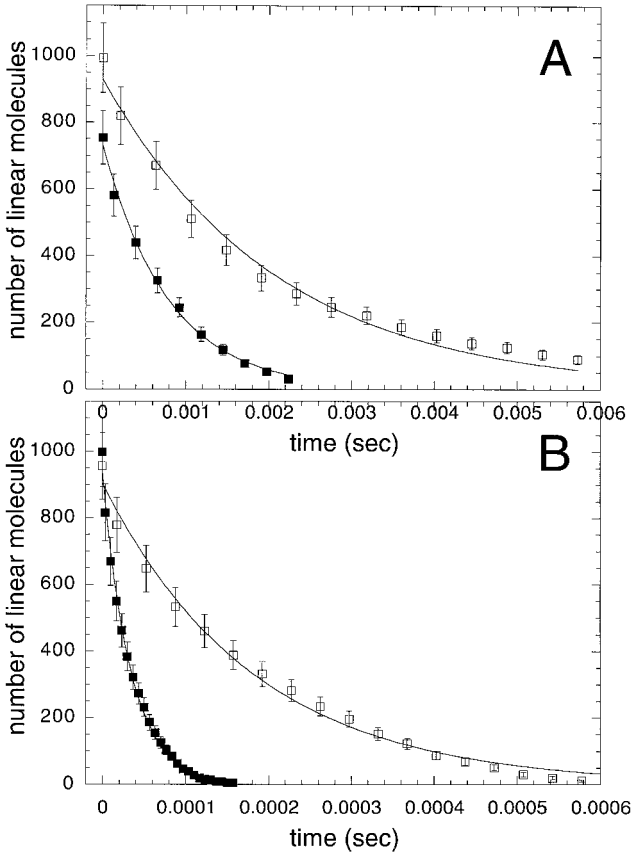

FIGURE 4 Kinetics of loop formation for $r = 10$ nm. The curves were fitted to the equation for a irreversible first-order reaction (Eq. 3) from which the rate constant for loop formation k_{on} could be determined (see also Table 1). (*A*) Straight fragments of 80 nm (—■—) and 160 nm (—□—) length. (*B*) DNAs with a central 120° DNA bend of 80 nm (—■—), and 160 nm (—□—).

TABLE 1 Parameters for loop formation at $r = 10$ nm

	80 nm, straight	80 nm, 120°	160 nm, straight	160 nm, 120°
j_M (M)	$3.0 \cdot 10^{-8}$	$2.2 \cdot 10^{-6}$	$1.0 \cdot 10^{-7}$	$4.5 \cdot 10^{-7}$
K^*_{eq}	$7.6 \cdot 10^{-5}$	$5.6 \cdot 10^{-3}$	$2.5 \cdot 10^{-4}$	$1.1 \cdot 10^{-3}$
k_{on} (s^{-1})#	$1.3 \cdot 10^{3}$	$3.0 \cdot 10^{4}$	$4.8 \cdot 10^{2}$	$5.5 \cdot 10^{3}$
k_{off} (s^{-1})§	$1.7 \cdot 10^{7}$	$5.4 \cdot 10^{6}$	$1.9 \cdot 10^{6}$	$4.8 \cdot 10^{6}$
$1/k_{on}$ (s)¶	$7.7 \cdot 10^{-4}$	$3.4 \cdot 10^{-5}$	$2.1 \cdot 10^{-3}$	$1.8 \cdot 10^{-4}$
$1/k_{off}$ (s)‖	$5.9 \cdot 10^{-8}$	$1.9 \cdot 10^{-7}$	$5.3 \cdot 10^{-7}$	$2.0 \cdot 10^{-7}$
$\ln 2/k_{on}$ (s)**	$5.5 \cdot 10^{-4}$	$2.3 \cdot 10^{-5}$	$1.4 \cdot 10^{-3}$	$1.2 \cdot 10^{-4}$

*The equilibrium constant for loop formation K_{eq} was calculated from j_M (see text).
#The rate constant for loop formation k_{on} was determined from Eq. 3.
§The rate constant for loop dissociation k_{off} was calculated from K_{eq} and k_{on}.
¶The average time it takes until the ends contact each other is given by $1/k_{on}$.
‖The average time the ends are within the contact distances $r = 10$ nm is given by $1/k_{off}$.
**The half-life, i.e., the time it takes until 50% of the molecules have approached each other to the contact distance $r = 10$ nm, is given by $\ln 2/k_{on}$.

loop also occurs, i.e., the reaction is reversible:

$$\text{linear} \underset{k_{off}}{\overset{k_{on}}{\rightleftharpoons}} \text{loop} \tag{4}$$

From the values of j_M that describe the equilibrium conformation for a given DNA fragment we can determine the equilibrium constant for the reaction shown above according to the following rationale: a contact probability of $p = 1$ would mean that one end is always located within a sphere of $r = 10$ nm around the other end. This is equal to a local concentration of $j_M = 4.0 \cdot 10^{-4}$ M and constitutes the upper limit for the value of j_M. Accordingly, the values of j_M determined for various DNA fragments can be converted into the probability p_{loop} to find the ends within $r = 10$ nm by using the value of $4.0 \cdot 10^{-4}$ M for $p = 1$. With p_{loop} the equilibrium constant for loop formation was then calculated from $K_{eq} = p_{loop}/(1 - p_{loop})$ and the off rate k_{off} for dissociation from $K_{eq} = k_{on}/k_{off}$. These values are given in Table 1.

DISCUSSION

We have measured the distribution and dynamics of the end-to-end distances of linear DNA chains ranging between 120 and 470 bp in length by using a Brownian dynamics model (Klenin et al., 1998). The data allow us to compute the Jacobson-Stockmayer factor, j_M (Jacobson and Stockmayer, 1950) for a cyclization reaction where the ends of the chain come into direct contact ($r = 0$) in good agreement with the analytical treatment by Shimada and Yamakawa (Shimada and Yamakawa, 1984) and results from cyclization experiments (Shore et al., 1981). This indicates that the equilibrium conformation of the linear DNAs is described adequately by the model. Beyond the simple case of a chain closing the circle at $r = 0$, numerical methods must be employed. We have used our model to compute j_M for the hypothetical case where two proteins bridge the two chain ends and keep them at a distance of $r = 10$ nm. The protein bridge in cooperation with an intrinsic DNA bend increases the loop formation probability for short DNA fragments (120–250 basepairs) by 3 to 5 orders of magnitude. We also showed that an asymmetric 80° bend as induced by TBP increases the interaction probability ~10-fold. One can conclude that bent DNA sequences between upstream binding elements and promoters are important for establishing—in cooperation with TBP—the contact between a transcription factor and the transcription complex at the promoter. The asymmetric bend assumed for the TBP has, however, a smaller effect on the cyclization probability than a symmetric bend located in the center between the two sites.

In the context of a longer DNA, one should consider that the j_M value for end-to-end interactions will be higher than for site-to-site interactions (Fig. 3). The "extra" DNA reduces the contact probability because it excludes certain conformations (in particular those with small r). Thus the j_M values here give an upper limit for the local concentration of site-to-site interactions.

In this work we could give, for the first time, an estimate of the effect of DNA bending and protein/DNA interaction on the kinetics of loop formation. From the data presented several important conclusions can be made for the interaction of DNA-bound proteins via looping of the DNA. For the short straight DNA a relative high value of $k_{on} = 1.3 \cdot 10^3$ was found as compared to its K_{eq} or j_M. This means that a short separation distance can be more effective in promoting protein-protein interactions than one would expect from the j_M value, if the proteins would make the reaction irreversible, i.e., almost every (also the short) contacts lead to an successful encounter. This might be an important finding in terms of the location of the upstream activation elements of eukaryotic promoters, which are generally located 100–200 bp away from the promoter.

Typical association rates for the DNA binding of eukaryotic transcription factors are in the order of 10^5 to 10^6 M^{-1} s^{-1} (Affolter et al., 1990; Carlsson and Haggblad, 1995; Hoopes et al., 1992). Since the intracellular concentration of these proteins is $\sim 10^{-8}$ to 10^{-9} M, this corresponds to a pseudo-first-order constant for the initial rate of complex formation between 10^{-2} and 10^{-4} s^{-1}. The rate k_{loop} for loop formation of the linear DNAs studied here was found to be $5 \cdot 10^2$ to $3 \cdot 10^4$ s^{-1}. This shows that the rate of loop formation is several orders of magnitude higher than the rate of protein binding. Thus, looping is unlikely to represent a rate-limiting step in the activation process, even if one considers an increase of the protein binding rate by sliding or other mechanisms of facilitated (one- or two-dimensional) diffusion on nonspecific DNA. However, since k_{loop} can vary by at least two orders of magnitude for different DNA conformations, it might very well be an important parameter in explaining why the effect of transcriptional enhancers is often restricted to a certain promoter.

REFERENCES

Affolter, M., A. Percival-Smith, M. Müller, W. Leupin, and W. J. Gehring. 1990. DNA binding properties of the purified Antennapedia homeodomain. *Proc. Natl. Acad. Sci. U.S.A.* 87:4093–4097.

Allison, S. A., R. Austin, and M. Hogan. 1989. Bending and twisting dynamics of short linear DNAs—analysis of the triplet anisotropy decay of a 209-base pair fragment by Brownian simulation. *J. Chem. Phys.* 90:3843–3854.

Allison, S. A., S. S. Sorlie, and R. Pecora. 1990. Brownian dynamics simulations of wormlike chains: dynamic light scattering from a 2311 base pair DNA fragment. *Macromolecules.* 23:1110–1118.

Beachy, P. A., J. Varkey, K. E. Young, D. P. von Kessler, B. I. Sun, and S. C. Ekker. 1993. Cooperative binding of an Ultrabithorax homeodomain protein to nearby and distant DNA sites. *Mol. Cell. Biol.* 13: 6941–6956.

Bednar, J., P. Furrer, A. Stasiak, J. Dubochet, E. H. Egelman, and A. D. Bates. 1994. The twist, writhe and overall shape of superhelical DNA change during counterion-induced transition from a loosely to a tightly interwound superhelix. Possible implications for DNA structure in vivo. *J. Mol. Biol.* 235:825–847.

Bellomy, G. R., M. C. Mossing, and M. T. Record. 1988. Physical properties of DNA in vivo as probed by the length dependence of the lac operator looping process. *Biochemistry.* 27:3900–3906.

Bellomy, G. R., and M. T. Record. 1990. Stable DNA loops in vivo and in vitro: roles in gene regulation at a distance and in biophysical characterization of DNA. *Prog. Nucleic Acid Res.* 39:81–128.

Borowiec, J. A., L. Zhang, S. Sasse-Dwight, and J. D. Gralla. 1987. DNA supercoiling promotes formation of a bent repression loop in lac DNA. *J. Mol. Biol.* 196:101–111.

Bracco, L., D. Kotlarz, A. Kolb, S. Diekmann, and H. Buc. 1989. Synthetic DNA curved sequences can act as transcriptional activators in *E. coli*. *EMBO J.* 8:4289–4296.

Carlsson, B., and J. Haggblad. 1995. Quantitative determination of DNA-binding parameters for the human estrogen receptor in a solid-phase, nonseparation assay. *Anal. Biochem.* 232:172–179.

Carmona, M., and B. Magasanik. 1996. Activation of transcription of σ^{54}-dependent promoters on linear templates requires intrinsic or induced bending of the DNA. *J. Mol. Biol.* 261:348–356.

Chirico, G., and J. Langowski. 1992. Calculating hydrodynamic properties of DNA through a second-order Brownian dynamics algorithm. *Macromolecules.* 25:769–775.

Chirico, G., and J. Langowski. 1994. Kinetics of DNA supercoiling studied by Brownian dynamics simulation. *Biopolymers.* 34:415–433.

Chirico, G., and J. Langowski. 1996. Brownian dynamics simulations of supercoiled DNA with bent sequences. *Biophys. J.* 71:955–971.

Ehrlich, L., C. Münkel, G. Chirico, and J. Langowski. 1997. A Brownian dynamics model for the chromatin fiber. *Computer Applications in the Biosciences*. 13:271–279.

Frappier, L., K. Goldsmith, and L. Bendell. 1994. Stabilization of the EBNA1 protein on the Epstein-Barr virus latent origin of DNA replication by a DNA looping mechanism. *J. Biol. Chem.* 269:1057–1062.

Frappier, L., and M. O'Donnell. 1991. Epstein-Barr nuclear antigen 1 mediates a DNA loop within the latent replication origin of Epstein-Barr virus. *Proc. Natl. Acad. Sci. U.S.A.* 88:10875–10879.

Gebe, J. A., S. A. Allison, J. B. Clendenning, and J. M. Schurr. 1995. Monte Carlo simulations of supercoiling free energies for unknotted and trefoil knotted DNAs. *Biophys. J.* 68:619–633.

Gebe, J. A., and J. M. Schurr. 1996. Thermodynamics of the first transition in writhe of a small circular DNA by Monte Carlo simulation. *Biopolymers.* 38:493–503.

Hagerman, P. J. 1988. Flexibility of DNA. *Annu. Rev. Biophys. Biophys. Chem.* 17:265–286.

Hagerman, P. J., and V. A. Ramadevi. 1990. Application of the method of phage T4 DNA ligase catalyzed ring-closure to the study of DNA structure. I. Computational analysis. *J. Mol. Biol.* 212:351–362.

Hagerman, P. J., and B. H. Zimm. 1981. Monte Carlo approach to the analysis of the rotational diffusion of wormlike chains. *Biopolymers.* 20:1481–1502.

Haykinson, M. J., and R. C. Johnson. 1993. DNA looping and the helical repeat in vitro and in vivo: effect of HU protein and enhancer location on Hin invertasome assembly. *EMBO J.* 12:2503–2512.

Heath, P. J., J. A. Gebe, S. A. Allison, and J. M. Schurr. 1996. Comparison of analytical theory with Brownian dynamics simulations for small linear and circular DNAs. *Macromolecules.* 29:3583–3596.

Hochschild, A. 1990. Protein-protein interactions and DNA loop formation. *In* DNA Topology and Its Biological Effects. Cold Spring Harbor Laboratory Press, Cold Spring Harbor, New York. 107–138.

Hoopes, B. C., J. F. LeBlanc, and D. K. Hawley. 1992. Kinetic analysis of yeast TFIID-TATA box complex formation suggests a multi-step pathway. *J. Biol. Chem.* 267:11539–11547.

Jacobson, H., and W. H. Stockmayer. 1950. Intramolecular reaction in polycondensations. I. The theory of linear systems. *J. Chem. Phys.* 18:1600–1606.

Kim, J. L., D. B. Nikolov, and S. K. Burley. 1993a. Co-crystal structure of TBP recognizing the minor groove of a TATA element. *Nature.* 365: 520–527.

Kim, Y., J. H. Geiger, S. Hahn, and P. B. Sigler. 1993b. Crystal structure of a yeast TBP/TATA-box complex. *Nature.* 365:512–520.

Klenin, K., M. D. Frank-Kamenetskii, and J. Langowski. 1995. Modulation of intramolecular interactions in superhelical DNA by curved sequences. A Monte Carlo simulation study. *Biophys. J.* 68:81–88.

Klenin, K., H. Merlitz, and J. Langowski. A Brownian dynamics program for the simulation of linear and circular DNA, and other wormlike chain polyelectrolytes. *Biophys. J.* 74:000–000. **Companion article 2881.**

Klenin, K. V., A. V. Vologodskii, V. V. Anshelevich, V. Y. Klishko, A. M. Dykhne, and M. D. Frank-Kamenetskii. 1991. Computer simulation of DNA supercoiling. *J. Mol. Biol.* 217:413–419.

Krämer, H., M. Niemöller, M. Amouyal, B. Révet, B. von Wilcken-Bergmann, and B. Müller-Hill. 1987. lac Repressor forms loops with linear DNA carrying two suitably spaced lac operators. *EMBO J.* 6:1481–1491.

Kremer, W., K. Klenin, S. Diekmann, and J. Langowski. 1993. DNA curvature influences the internal motion of superhelical DNA. *EMBO J.* 12:4407–4412.

Langowski, J., U. Kapp, K. Klenin, and A. Vologodskii. 1994. Solution structure and dynamics of DNA topoisomers. Dynamic light scattering studies and Monte Carlo simulations. *Biopolymers.* 34:639–646.

Langowski, J., W. K. Olson, S. C. Pedersen, I. Tobias, T. P. Westcott, and Y. Yang. 1996. DNA supercoiling, localized bending and thermal fluctuations. *Trends Biochem. Sci.* 21:50.

Laundon, C. H., and J. D. Griffith. 1988. Curved helix segments can uniquely orient the topology of supertwisted DNA. *Cell.* 52:545–549.

Lavigne, M., M. Herbert, A. Kolb, and H. Buc. 1992. Upstream curved sequences influence the initiation of transcription at the *Escherichia coli* galactose operon. *J. Mol. Biol.* 224:293–306.

Law, S. M., G. R. Bellomy, P. J. Schlax, and M. T. Record. 1993. In vivo thermodynamic analysis of repression with and without looping in lac constructs. Estimates of free and local lac repressor concentrations and of physical properties of a region of supercoiled DNA in vivo. *J. Mol. Biol.* 230:161–173.

Lewis, M., G. Chang, N. C. Horton, M. A. Kercher, H. C. Pace, M. A. Schumacher, R. G. Brennan, and P. Lu. 1996. Crystal structure of the lactose operon repressor and its complexes with DNA and inducer. *Science.* 271:1247–1254.

Martino, J. A., and W. K. Olson. 1997. Modeling protein-induced configurational changes in DNA minicircles. *Biopolymers.* 41:419–430.

Moitoso de Vargas, L., S. Kim, and A. Landy. 1989. DNA looping generated by DNA bending protein IHF and the two domains of lambda integrase. *Science.* 244:1457–1461.

Mossing, M. C., and M. T. Record. 1986. Upstream operators enhance repression of the lac-promoter. *Science.* 233:889–892.

Olson, W. K. 1996. Simulating DNA at low resolution. *Curr. Opin. Struct. Biol.* 6:242–256.

Olson, W. K., N. L. Marky, R. L. Jernigan, and V. B. Zhurkin. 1993. Influence of fluctuations on DNA curvature. *J. Mol. Biol.* 232:530–554.

Rippe, K., M. Guthold, P. H. von Hippel, and C. Bustamante. 1997. Transcriptional activation via DNA-looping: visualization of intermedi-

ates in the activation pathway of *E. coli* RNA polymerase · σ^{54} holoenzyme by scanning force microscopy. *J. Mol. Biol.* 270:125–138.

Rippe, K., P. H. von Hippel, and J. Langowski. 1995. Action at a distance: DNA-looping and initiation of transcription. *Trends Biochem. Sci.* 20: 500–506.

Rybenkov, V. V., A. V. Vologodskii, and N. R. Cozzarelli. 1997a. The effect of ionic conditions on DNA helical repeat, effective diameter and free energy of supercoiling. *Nucleic Acids Res.* 25:1412–1418.

Rybenkov, V. V., A. V. Vologodskii, and N. R. Cozzarelli. 1997b. The effect of ionic conditions on the conformations of supercoiled DNA. 1. Sedimentation analysis. *J. Mol. Biol.* 267:299–311.

Santero, E., T. R. Hoover, A. K. North, D. K. Berger, S. C. Porter, and S. Kustu. 1992. Role of integration host factor in stimulating transcription from the σ^{54}-dependent nifH promoter. *J. Mol. Biol.* 227:602–620.

Schleif, R. 1992. DNA looping. *Annu. Rev. Biochem.* 61:199–223.

Schlick, T., and W. K. Olson. 1992. Supercoiled DNA energetics and dynamics by computer simulation. *J. Mol. Biol.* 223:1089–1119.

Shimada, J., and H. Yamakawa. 1984. Ring-closure probabilities of twisted wormlike chains. Application to DNA. *Macromolecules.* 17:689–698.

Shore, D., and R. L. Baldwin. 1983. Energetics of DNA twisting. I. Relation between twist and cyclization probability. *J. Mol. Biol.* 179: 957–981.

Shore, D., J. Langowski, and R. L. Baldwin. 1981. DNA flexibility studied by covalent closure of short fragments into circles. *Proc. Natl. Acad. Sci. U.S.A.* 78:4833–4837.

Stenger, J. E., P. Tegtmeyer, G. A. Mayr, M. Reed, Y. Wang, P. Wang, P. V. Hough, and I. A. Mastrangelo. 1994. p53 oligomerization and DNA looping are linked with transcriptional activation. *EMBO J.* 13: 6011–6020.

Su, W., T. Middleton, B. Sugden, and H. Echols. 1991. DNA looping between the origin of replication of Epstein-Barr virus and its enhancer site: stabilization of an origin complex with Epstein-Barr nuclear antigen 1. *Proc. Natl. Acad. Sci. U.S.A.* 88:10870–10874.

Su, W., S. Porter, S. Kustu, and H. Echols. 1990. DNA-looping and enhancer activity: association between DNA-bound NtrC activator and RNA polymerase at the bacterial glnA promoter. *Proc. Natl. Acad. Sci. U.S.A.* 87:5504–5508.

Vologodskii, A. V., S. D. Levene, K. V. Klenin, M. D. Frank-Kamenetskii, and N. R. Cozzarelli. 1992. Conformational and thermodynamic properties of supercoiled DNA. *J. Mol. Biol.* 227:1224–1243.

Wedel, A., D. S. Weiss, D. Popham, P. Dröge, and S. Kustu. 1990. A bacterial enhancer functions to tether a transcriptional activator near a promoter. *Science.* 248:486–490.

Yang, Y., T. P. Westcott, S. C. Pedersen, I. Tobias, and W. K. Olson. 1995. Effects of localized bending on DNA supercoiling. *Trends Biochem. Sci.* 20:313–319.

Zhang, P. S., I. Tobias, and W. K. Olson. 1994. Computer simulation of protein-induced structural changes in closed circular DNA. *J. Mol. Biol.* 242:271–290.